(Received 24 June 2023, Accepted 30 November 2023, Scheduled 13 December 2023)

Non-Singular Fast Terminal Sliding Mode Control Torsional Vibration Suppression for PM Synchronous Transmission System of EVs

Ning Jia, Kaihui Zhao*, Yuying Lv, and Xiangfei Li

College of Electrical and Information Engineering, Hunan University of Technology, China

ABSTRACT: To suppress the torsional vibration caused by the omission of couplings and dampers during flexible power transmission in the permanent magnet (PM) synchronous drive system of pure electric vehicles (EVs), this paper presents a non-singular fast terminal sliding mode control (NFTSMC) torsional vibration suppression strategy based on a sliding mode disturbance observer (SMDO). First, a PM synchronous drive system is simplified as a two-inertia model, and a mathematical model is established. Then, an NFTSMC controller of the load-side speed feedback is designed to suppress torsional vibration. Meanwhile, an SMDO is designed to estimate the load disturbance, and the estimated value is fed back to the controller to perform feedforward compensation. The robustness of the system is improved, and the effect of the load disturbance on the system is reduced. The results of the simulations and experiments show that the presented NFTSMC based on the SMDO strategy has a strong torsional vibration suppression effect compared to PI control and conventional sliding mode control.

1. INTRODUCTION

In recent years, new energy vehicles have captured the most of the automotive market due to their high energy conversion efficiency, environmental friendliness, and green credentials. The clean, efficient, and emission-free nature of electric vehicles (EVs) have made them a popular choice for solving air pollution problems. It is important for achieving peak carbon emissions and carbon neutrality [1–3]. Today's vehicles are meeting higher demands for economy and performance. However, driveline's torsional vibrations are getting worse, which affects overall vehicle performance. The resulting noise, vibration, and harshness (NVH) problems also reduce passenger comfort. Therefore, it is essential to analyze and study torsional vibration in EVs. Torsional vibration has long been concerned about in vehicles with internal combustion engine vehicles [4]. The problem is even more serious in pure electric and hybrid electric vehicles. The first reason is the lack of damping components, such as clutches, torsional dampers, and torque converters; the second reason is the rapid torque rise time of the engine, which triggers torsional resonance [5]. Torsional vibration problems in transmission systems already exist in industrial applications, such as rolling mills, servo motor control, or similar multi-mass systems. In such systems, torsional resonance frequencies exist as a function of motor and load inertia and shaft stiffness [6–9].

The integrated powertrain of an EV is a nonlinear, highly uncertain complex system in which the permanent magnet synchronous motor (PMSM), driveline, and control system are electro-mechanically coupled [10]. Estimation, control, and optimization are the three main technical challenges of electrified powertrains. In terms of control and performance optimization, the EVs powertrain has a simple structure with few running and transmission components. In fact, the low-damping characteristic of the motor makes the torque and speed control of the motor quickly, which significantly improves the transmission efficiency and power density of the powertrain, thus contributing to the lightweight of EVs. However, motor controller is usually designed to generate the required torque regardless of the mechanical state, and the load side and motor side generate angular shifts. Thus, it causes torsional vibration problems in EVs. A torsional vibration control method combining a dimensional reduction observer and Linear Quadratic Regulator (LQR) is proposed for an integrated EV powertrain to achieve powertrain torsional vibration suppression [11]. A new algorithm is proposed for the simultaneous identification of powertrain tooth gap position and half-shaft torque, and the road test data of highly dynamic vehicle state changes were verified by using a hybrid state observer [12]. However, the algorithm is too complex and difficult to implement in engineering. A powertrain model of an EV with a two-speed transmission has been developed in [13]. The effects on free and forced vibrations were analyzed in terms of torsional stiffness and damping coefficients, but the influence of other parameters on the system was not considered.

Due to the advantages of high reliability and efficiency, high overload capacity, high power density, and high torque to weight ratio, PMSMs for vehicles have dominated the market of EV drive motors. Compared to reluctance motors, PMSMs produce less torque pulsation and noise, which provides a new

* Corresponding author: Kaihui Zhao (zhaokaihui@hut.edu.cn).

direction for solving NVH problems in EVs. At present, the dual proportional-integral (PI) control technique of speed external loop-current internal loop has become the mainstream control method for electric motors due to the advantages of simple algorithms and easy engineering implementation. However, in the actual electromechanical coupling system, the electromagnetic force effect is transferred directly between the motor rotor and drive shaft. This results in a high frequency of torque fluctuations, which is more likely to have an impact on the drive system and lead to unsatisfactory control performance.

For the control requirements of PMSM in EVs, many advanced control methods are widely used, such as model predictive control [14], state feedback control [15], active disturbance rejection control (ADRC) [16], and sliding mode control (SMC). Among them, SMC is considered as one of the most effective methods to improve the immunity and robustness of PMSM systems and has attracted much attention. A model-free sliding mode controller with an extended sliding mode disturbance observer was designed to estimate the unknown part of the ultra-local model, which effectively improved the dynamic performance of the PMSM and ensured the strong robustness of the system [17]. A model-free non-singular terminal sliding mode combined with an extended non-singular sliding mode disturbance observer is proposed, and the speed-loop controller is designed, which reduces the dependence on the mathematical model of the motor, but the parameter regulation is complex and not very practical [18].

At present, the research on torsional vibration controllers for pure EVs mainly involves the design of a notch filter to reduce the amplitude of the conjugate pole depression peaks of the system transfer function and to reduce the oscillations in the system. A novel multi-notch filters (MNFs) method with a frequency estimator is presented to suppress the harmonic vibration for maglev rotor system [19]. A Butterworth low-pass filter is designed to suppress local vibration for PMSM Servo System [20]. A vibration compensation control method based on an adaptive neural network band-pass filter (ANNBPF) is proposed to solve the problem of rotor vibration for the bearingless PMSM [21].

This paper innovatively presents a sliding mode control method from the control perspective to solve the torsional vibration problem of EVs by designing a sliding mode torsional vibration controller. The method is based on a simplified two-inertia model of the permanent magnet (PM) synchronous drive system and the design of a non-singular fast terminal sliding mode controller (NFTSMC) to suppress torsional vibration. A sliding mode disturbance observer (SMDO) is also designed to accurately estimate the load disturbance of the system in real time and perform feedforward compensation for NFTSMC. This effectively improves the anti-disturbance capability of the closed-loop motor drive control system and achieves effective torsional vibration suppression in the PM synchronous drive system. The correctness and effectiveness of the presented control algorithm were verified by simulations, experiments, and a comprehensive comparison with PI control and conventional sliding mode control algorithms.

The contributions of this study are summarized as follows:

(i) An NFTSMC based on the SMDO method is presented to effectively suppress torsional vibration and improve the anti-disturbance capability of EVs.

(ii) An SMDO is designed to accurately estimate the load disturbance and perform feedforward compensation for NFTSMC.

(iii) Through simulations and experiments, the effectiveness of the presented control algorithm is verified by comparing with PI control and conventional SMC.

This paper is structured as follows. The system description is presented in Section 2. In Section 3, an NFTSMC based on the SMDO is designed to achieve torsional vibration suppression of the PM synchronous drive system. Section 4 exhibits the results of simulations and experiments. Finally, conclusions are given.

2. SYSTEM DESCRIPTION

2.1. Mathematical Model of PMSM

Ignoring stator core saturation, parameter perturbation, and hysteresis loss, the stator voltage equation of PMSM in the *d-q* axis coordinate is expressed as:

$$\begin{cases} u_d = R_s i_d + \dfrac{d}{dt}\psi_d - \omega_e L_q i_q \\ u_q = R_s i_q + \dfrac{d}{dt}\psi_q + \omega_e \left(L_d i_d + \psi_f\right) \end{cases} \tag{1}$$

where L_d, L_q are the *d-q* axis inductances (H); i_d, i_q are the *d-q* axis stator currents (A); u_d, u_q are the *d-q* axis stator voltages (V); R_s is the stator resistance (Ω); ψ_f is the permanent magnet fluxlinkage (Wb); ω_e is the electric angular velocity (rad/s); ψ_d, ψ_q are the *d-q* axis stator magnet flux component (Wb), respectively.

The electromagnetic torque equation of PMSM is expressed as:

$$\begin{aligned} T_e &= 1.5 n_p (\psi_d i_q - \psi_q i_d) \\ &= 1.5 n_p \left[\psi_f i_q + (L_d - L_q)\, i_d i_q\right] \end{aligned} \tag{2}$$

where T_e is the electromagnetic torque (N $\cdot$ m); n_p is the pole number (pairs).

The inductance of a surface-mounted PMSM (SPMSM) satisfies $L_d = L_q = L$. As a result, the SPMSM torque is independent of the *d*-axis current and is only linearly related to the *q*-axis current. The electromagnetic torque equation is:

$$T_e = n_p \psi_f i_q \tag{3}$$

The mechanical motion equation of SPMSM is:

$$J\frac{d\omega_M}{dt} = T_e - T_L - B\omega_M \tag{4}$$

where T_L is the load torque (N $\cdot$ m); B is the viscous friction coefficient (N $\cdot$ m $\cdot$ s); ω_M is the mechanical angular speed of the motor (rad/s) and satisfies $\omega_M = \omega_e / n_p$; J is the rotational inertia of the system ($kg \cdot \mathrm{m}^2$). Assuming that the motor and

load are ideally connected by a rigid shaft, and the rotational inertia of the motor and the load are J_M and J_L, $J = J_M + J_L$.

According to (1), (3), and (4), the state equation of the SPMSM is obtained

$$\begin{cases} \dfrac{di_d}{dt} = -\dfrac{R_s}{L} i_d + n_p \omega_M i_q + \dfrac{u_d}{L} \\ \dfrac{di_q}{dt} = -n_p \omega_M i_d - \dfrac{R_s}{L} i_q - \dfrac{n_p \psi_f}{L} \omega_M + \dfrac{u_q}{L} \\ \dfrac{d\omega_M}{dt} = \dfrac{n_p \psi_f}{J} i_q - \dfrac{B}{J} \omega_M - \dfrac{T_L}{J} \\ \dfrac{d\theta_M}{dt} = \omega_M \end{cases} \tag{5}$$

where θ_M is the mechanical angular position of the motor rotor and satisfies $\theta_M = \theta_e / n_p$.

2.2. Simplified Model of Pure Electric Vehicle Drivetrain

The general structure of a PM traction system of an EV is shown in Fig. 1. The powertrain consists of a PMSM, a gearbox, a main gearbox, a differential and two half shafts. The motor is mounted in the center of the front axle of the vehicle. During acceleration and cruising, the motor provides the torque which is transmitted through the driveline and applied to the axles to keep the car moving. The powertrain analyzed in this paper has a central drive topology that does not take into account the nonlinear characteristics, and it is abstracted as a simplified two-inertia model. For simplicity, the model does not include gear backlash, and the change in mesh stiffness during transmission and ignores the differential speed effect of the reducer. The output torque of the engine is assumed to be transferred equally to the left and right half shafts [22].

The state equation of the pure EV is

$$\begin{cases} \dfrac{di_d}{dt} = -\dfrac{R_s}{L} i_d + n_p \omega_M i_q + \dfrac{u_d}{L} \\ \dfrac{di_q}{dt} = -n_p \omega_M i_d - \dfrac{R_s}{L} i_q - \dfrac{n_p \psi_f}{L} \omega_M + \dfrac{u_q}{L} \\ \dfrac{d\omega_M}{dt} = \dfrac{n_p \psi_f}{J_M} i_q - \dfrac{b_s}{J_M} (\omega_M - \omega_L) - \dfrac{K_s}{J_M} (\theta_M - \theta_L) \\ \dfrac{d\omega_L}{dt} = -\dfrac{b_s}{J_L} (\omega_M - \omega_L) - \dfrac{K_s}{J_L} (\theta_M - \theta_L) - \dfrac{T_L}{J_L} \\ \dfrac{d\theta_M}{dt} = \omega_M \\ \dfrac{d\theta_L}{dt} = \omega_L \end{cases} \tag{6}$$

where J_M is the rotational inertia of the driven PMSM; J_L is the equivalent rotational inertia of the wheel equivalent to the vehicle end; ω_M is the mechanical angular velocity of the motor; ω_L is the equivalent angular velocity of the vehicle end; K_s is the equivalent torsional stiffness of the half shaft and wheel equivalent to the vehicle end; b_s is the equivalent torsional damping; θ_M, θ_L are the angular position of the motor rotor and the load.

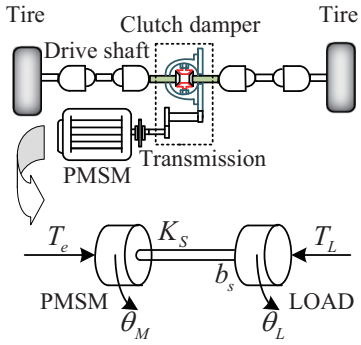

FIGURE 1. Simplified two-inertia model of EV.

3. TORSIONAL VIBRATION SUPPRESSION CONTROL

This section designs a sliding mode controller for a simplified model of an EV to achieve torsional vibration suppression. To avoid the integral saturation of PI controllers and the chattering problems of conventional SMC, a second-order non-singular fast terminal sliding mode (NFTSM) control method is used according to the load feedback speed.

3.1. Sliding Mode Torsional Vibration Control

The given load speed is ω_L^*, and the load speed error is chosen as the state variable:

$$\begin{cases} x_1 = \omega_L^* - \omega_L \\ \dot{x}_1 = x_2 \end{cases} \tag{7}$$

According to (7), the speed error equation is:

$$\begin{aligned} x_2 &= \dot{\omega}_L^* - \dot{\omega}_L \\ &= \dot{\omega}_L^* - \frac{b_s}{J_L} (\omega_M - \omega_L) - \frac{K_S}{J_L} (\theta_M - \theta_L) + \frac{T_L}{J_L} \end{aligned} \tag{8}$$

Since the load torque is a constant, the derivative of (8) gives:

$$\begin{aligned} \dot{x}_2 = &- \frac{b_s n_p \psi_f}{J_M J_L} i_q + \ddot{\omega}_L^* + \left(\frac{b_s^2}{J_P J_L} - \frac{K_S}{J_L} \right) (\omega_M - \omega_L) \\ &+ \frac{K_S b_s}{J_P J_L} (\theta_M - \theta_L) - \frac{b_s T_L}{J_L^2} \end{aligned} \tag{9}$$

where $\frac{1}{J_p} = \frac{1}{J_M} + \frac{1}{J_L}$. To effectively reduce the steady-state error, the NFTSM surface is selected as [23]:

$$s = x_1 + \alpha {x_1}^{l/h} + \beta {x_2}^{p/q} \tag{10}$$

where α, β are constants to be designed and are greater than zero. l, h, p, q are all constant odd numbers to be designed; $1 < p/q < 2$, $l/h > p/q$

The derivative of (10) gives:

$$\begin{aligned} \dot{s} &= x_2 + \frac{\alpha l}{h} x_1^{l/h-1} x_2 + \frac{\beta p}{q} x_2^{p/q-1} \dot{x}_2 \\ &= x_2 \left(1 + \frac{\alpha l}{h} x_1^{l/h-1} \right) + \frac{\beta p}{q} x_2^{p/q-1} \dot{x}_2 \end{aligned} \tag{11}$$

To eliminate the chattering caused by the sliding mode control and to speed up the convergence motion, the exponential convergence law is chosen as:

$$\dot{s} = -\varepsilon \text{sgn}(s) - ks \tag{12}$$

where $k > 0$, $\varepsilon > 0$ are the gains to be designed.

Combining (7)–(9), and (11)–(12), the output of NFTSMC is obtained as:

$$\begin{aligned} i_q = \frac{J_M J_L}{b_s n_p \psi_f} \Bigg[& \frac{q}{\beta p} x_2^{2-p/q} \left(1 + \frac{\alpha l}{h} x_1^{l/h-1}\right) + \ddot{\omega}_L^* \\ & + \left(\frac{b_s^2}{J_P J_L} - \frac{K_S}{J_L}\right)(\omega_M - \omega_L) + \frac{K_S b_s}{J_P J_L}(\theta_M - \theta_L) \\ & - \frac{b_s T_L}{J_L^2} + \varepsilon \text{sgn}(s) + ks \Bigg] \end{aligned} \tag{13}$$

Theorem 1 *If the NFTSM surface* (10) *is chosen, and the exponential convergence law* (12) *is chosen, the designed sliding mode controller* (13) *is asymptotically stable.*

Proof 1 *Consider Lyapunov functions as follows:*

$$V_1 = \frac{1}{2} s^2 \tag{14}$$

Take the derivative of V_1*:*

$$\begin{aligned} \dot{V} &= s\left(x_2 + \frac{\alpha l}{h} x_1^{l/h-1} x_2 + \frac{\beta p}{q} x_2^{p/q-1} \dot{x}_2\right) \\ &= s\left\{x_2\left(1 + \frac{\alpha l}{h} x_1^{l/h-1}\right) + \frac{\beta p}{q} x_2^{p/q-1} \right. \\ &\quad \left. \left[-\frac{q}{\beta p} x_2^{2-p/q}\left(1 + \frac{\alpha l}{h} x_1^{l/h-1}\right) - \varepsilon \text{sgn}(s) - ks\right]\right\} \\ &= s\left\{\frac{\beta p}{q} x_2^{p/q-1}\left[-\varepsilon \text{sgn}(s) - ks\right]\right\} \\ &= \frac{\beta p}{q} x_2^{p/q-1}\left[-\varepsilon |s| - ks^2\right] \\ &\le -\frac{\beta p}{q} x_2^{p/q-1} |s| \end{aligned} \tag{15}$$

where $1 < p/q < 2$, $0 < p/q - 1 < 1$, *p, q* ($p > q$) *are positive even numbers.*

From (15), $x_2^{p/q-1} > 0$, $\dot{V}_1 \le 0$. *According to Lyapunov's stability theorem, the system state will converge in finite time. The reachable condition of the sliding mode is satisfied. The designed sliding mode controller is asymptotically stable.*

3.2. Sliding Mode Disturbance Observer

The sliding mode disturbance observer (SMDO) is designed to estimate the load disturbance in real time by the input and output of the system. The feedforward compensation is performed on the NFTSMC.

The speed loop sliding mode disturbance observer (SMDO) is designed as:

$$\begin{cases} \dot{\hat{\omega}}_e = \dfrac{n_p \psi_f}{J} i_q - \dfrac{B}{J}\hat{\omega}_e - \dfrac{\hat{T}_L}{J} \\ \dot{\hat{T}}_L = l_1 u_{smo} \end{cases} \tag{16}$$

where $\hat{\omega}_e$ is the estimated speed; $\hat{T}_L$ is the observed load disturbance; $\dot{\hat{T}}_L$ represents its rate of change; u_{smo} is the sliding mode function to be designed; $l_1 > 0$ is the observer gain.

The observation error of (16) is expressed as:

$$\begin{cases} \dot{e}_\omega = -\dfrac{\tilde{T}_L}{J} - \dfrac{B}{J} e_\omega + u_{smo} \\ \dot{\tilde{T}}_L = l_1 u_{smo} \end{cases} \tag{17}$$

where $e_\omega = \hat{\omega}_e - \omega_e$ is the speed observation error; $\tilde{T}_L = \hat{T}_L - T_L$ is the estimation error of load disturbance.

u_{smo} is designed as:

$$u_{smo} = \gamma \text{sgn}(l) + \eta l \tag{18}$$

where γ, η are designed parameter numbers.

Theorem 2 *Selecting the sliding mode surface* $l = e_\omega$ *and choosing the appropriate observer gain* $\gamma \ge \left|\tilde{T}_L / J\right|$, *the state error* (16) *will converge to zero in finite time.*

Proof 2 *Consider Lyapunov functions as:*

$$V_2 = \frac{1}{2} l^2 \tag{19}$$

Take the derivative of V_2

$$\begin{aligned} \dot{V}_2 &= l\dot{l} \\ &= l\left[-\frac{B}{J} e_\omega - \frac{\tilde{T}_L}{J} + \gamma \text{sgn}(l) + \eta l\right] \\ &= -\frac{B l^2}{J} + \eta l^2 + l\left[-\frac{\tilde{T}_L}{J} + \gamma \text{sgn}(l)\right] \end{aligned} \tag{20}$$

where $J > 0$, $B > 0$. *When the stability condition is satisfied, it is simplified to*

$$\begin{aligned} \dot{V}_2 &\le -l\frac{\tilde{T}_L}{J} + l\gamma \text{sgn}(l) \\ &\le -l\frac{\tilde{T}_L}{J} + |l|\gamma \\ &\le -|l|\left(\frac{\tilde{T}_L}{J} - \gamma\right) \end{aligned} \tag{21}$$

When the gain $0 < \eta < \frac{B}{J}$ *and* $\gamma \ge \left|\frac{\tilde{T}_L}{J}\right|$ *are chosen,* $\dot{V}_2 \le 0$. *The SMDO is asymptotically stable.*

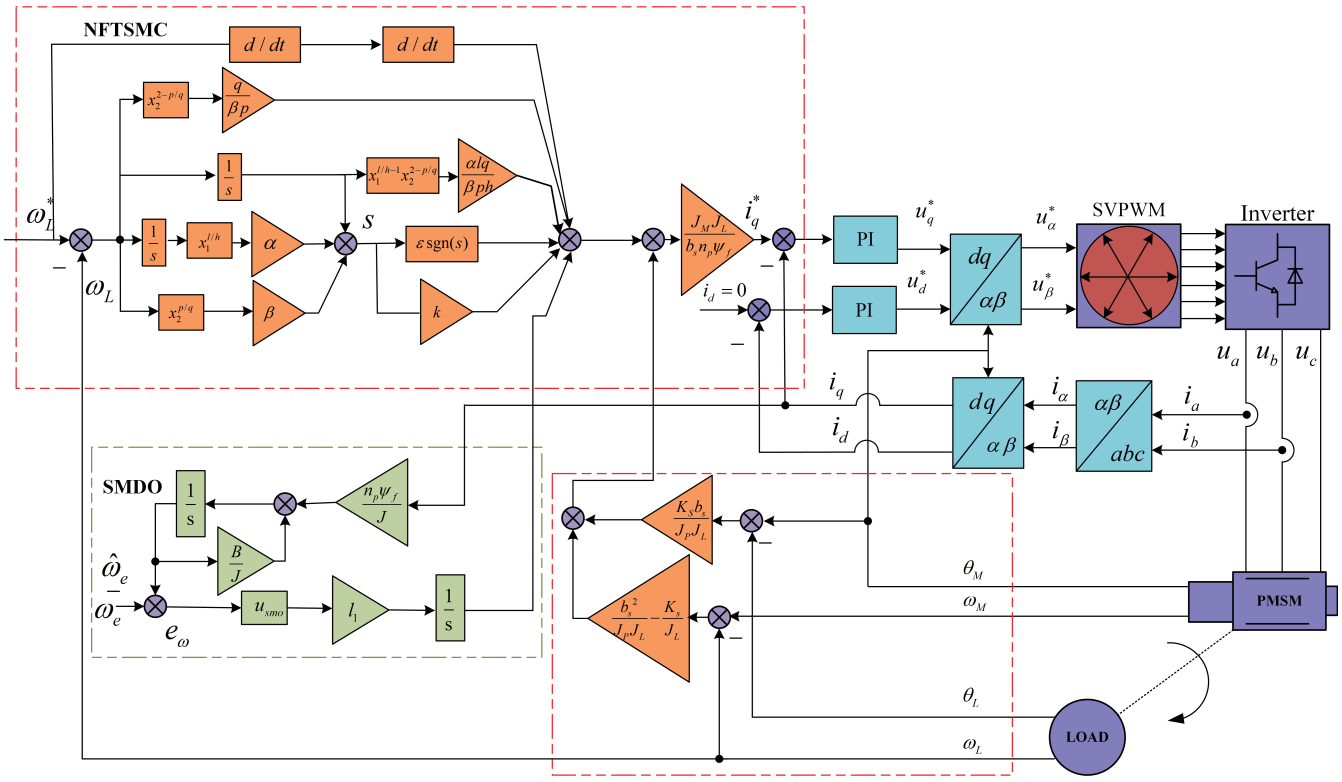

FIGURE 2. Simplified two-inertia model of EV.

TABLE 1. Parameters of PMSM.

Parameters	Unit	Values
DC side voltage U_{dc}	V	350
rotor PM flux (ψ_f)	Wb	0.171
stator inductance (L)	H	0.00334
stator resistance (R_s)	Ω	1.9
number of pole pairs (n_p)	pairs	4
Friction coefficient (B)	N · m · s/rad	0.0001
rotational inertia (J_M)	kg · m^2	0.015
Torsional stiffness (K_S)	N · m/rad	4000
Torsional damping (b_s)	N · m · s/rad	100
Overall vehicle inertia (J_L)	kg · m^2	2.5

TABLE 2. Parameters of three control methods.

PI	SMC	NFTSMC
$P = 1050$	$c = 550$	$\alpha = 12000$
$I = 32$	$\varepsilon = 500$	$\beta = 2000$
–	$k = 140$	$l/h = 7/3$
–	–	$p/q = 5/3$
–	–	$\varepsilon = 0.01$
–	–	$k = 0.008$
–	–	$\gamma = 200$
–	–	$\eta = 4000$
–	–	$l_1 = 62$

To reduce the chattering caused by the sliding-mode sign function, the saturation function sat (s) is used instead of the sign function. The saturation function sat (s) is:

$$\text{sat}\,(s) = \begin{cases} \text{sgn}\,(s) & |s| > \Delta \\ \frac{s}{\Delta} & |s| \le \Delta \end{cases} \tag{22}$$

where Δ is the value of the boundary layer.

Fig. 2 shows the block diagram of the proposed NFTSMC torsional vibration suppression system for EV. The proposed algorithm is shown in the red dashed box. The control process is as follows: first, the PMSM speed loop NFTSMC controller is designed according to the two-inertia model of the EV; then, the load disturbance is accurately observed by SMDO, and the observed value is fed back to the NFTSMC controller to achieve the suppression of the load-side torsional vibration.

4. SIMULATION AND EXPERIMENT

This section gives the results of the simulations and hardware-in-the loop simulation (HILS) experiments to verify the feasibility and effectiveness of the presented SMDO-based NFTSMC method. A two-inertia model of the pure EV is constructed using the MATLAB/Simulink. The proposed method is compared with PI control and conventional SMC.

The motor is controlled by using the $i_d = 0$ control strategy. The q-axis reference current is provided by an external speed loop controller. The sampling period is set to 10 µs, and the

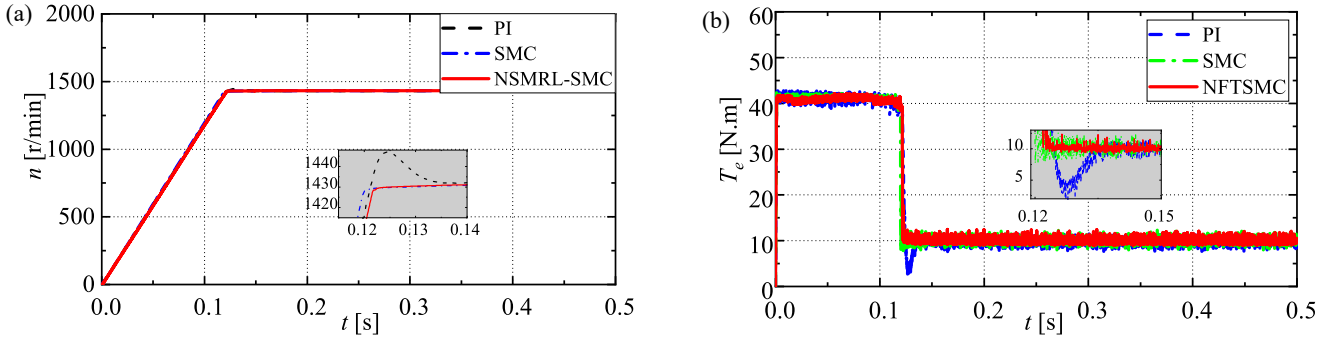

FIGURE 3. Simulation results of speed response, output torque by PI, SMC, and NFTSMC during acceleration and cruising. (a) n. (b) T_e.

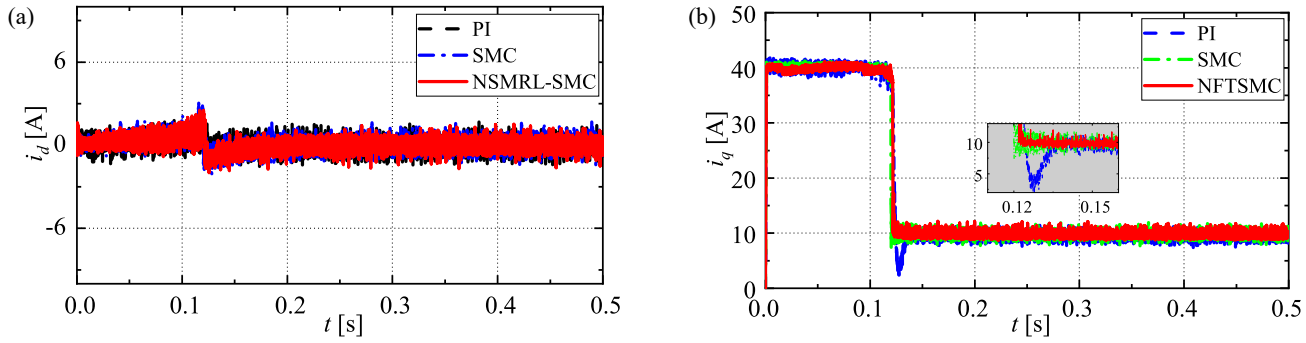

FIGURE 4. Simulation results of *d-q* axis current response by PI, SMC, and NFTSMC during acceleration and cruising. (a) i_d. (b) i_q.

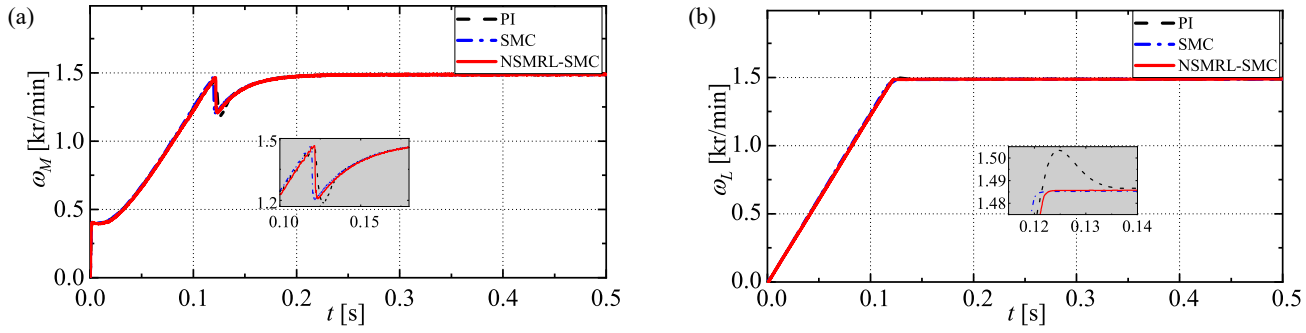

FIGURE 5. Simulation results of speed response at motor-side, load-side by PI, SMC and NFTSMC. (a) ω_M. (b) ω_L.

DC voltage is 350 V. The parameters of the PMSM are shown in Table 1. Table 2 shows the control parameters of the PI control, conventional SMC and NFTSMC. In the conventional SMC, the sliding mode surface is chosen as $s = cx_1 + x_2$, and the exponential convergence law is chosen as $\dot{s} = -\varepsilon_1 \mathrm{sgn}(s) - k_1 s$.

4.1. Simulation Results at Acceleration and Cruising Conditions

Figures 3 and 4 show the simulation comparison of the NFTSMC method with PI control and conventional SMC during the start-up, acceleration, and cruise of the EV. Fig. 3 shows the speed response waveform and motor output torque waveform. Fig. 4 shows the *d-q* axis current response waveform.

The speed variation curve in Fig. 3 shows that the NFTSMC reaches the reference speed at 0.12 s during the start-up, while the PI and SMC reach the steady state at 0.14 s and 0.13 s, respectively. The steady-state control accuracy of the NFTSMC is better than that of the PI and SMC.

It is clear from Fig. 4 that the convergence performance of PI control and conventional SMC is poor at speed steps, and the *d-q* axis current waveforms of NFTSMC are the smoothest with the least pulsation. The experiments show that the NFTSMC strategy has high transient steady state performance.

4.2. Simulation Results of Torsional Vibration Suppression

Figures 5 to 7 show the simulated comparison of NFTSMC with PI control and conventional SMC for the motor side and load side of the two-inertia system during start-up acceleration and

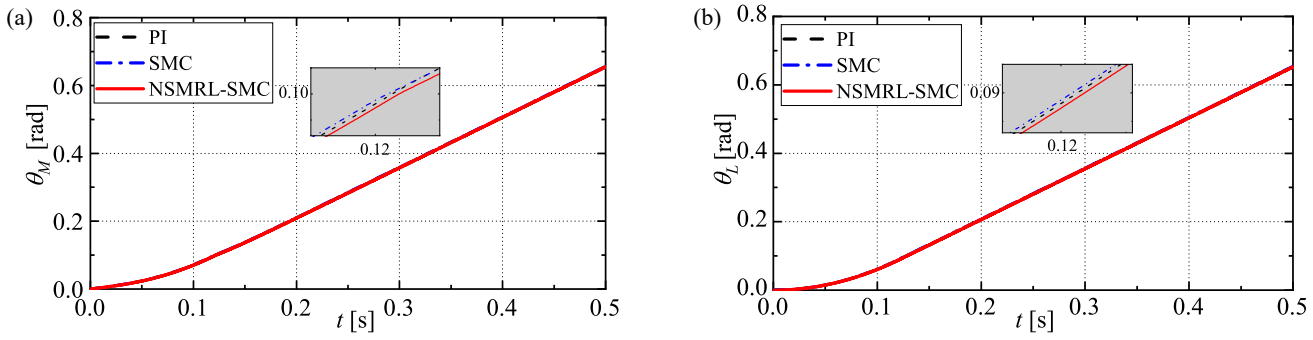

FIGURE 6. Simulation results of motor-side, load-side angle position by PI, SMC and NFTSMC. (a) θ_M. (b) θ_L.

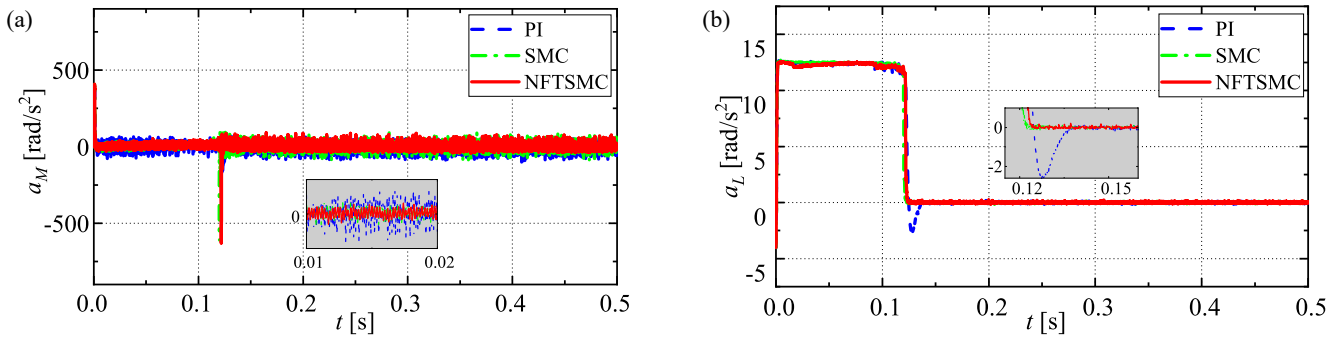

FIGURE 7. Simulation results of motor-side, load-side angle acceleration by PI, SMC and NFTSMC. (a) a_M. (b) a_L.

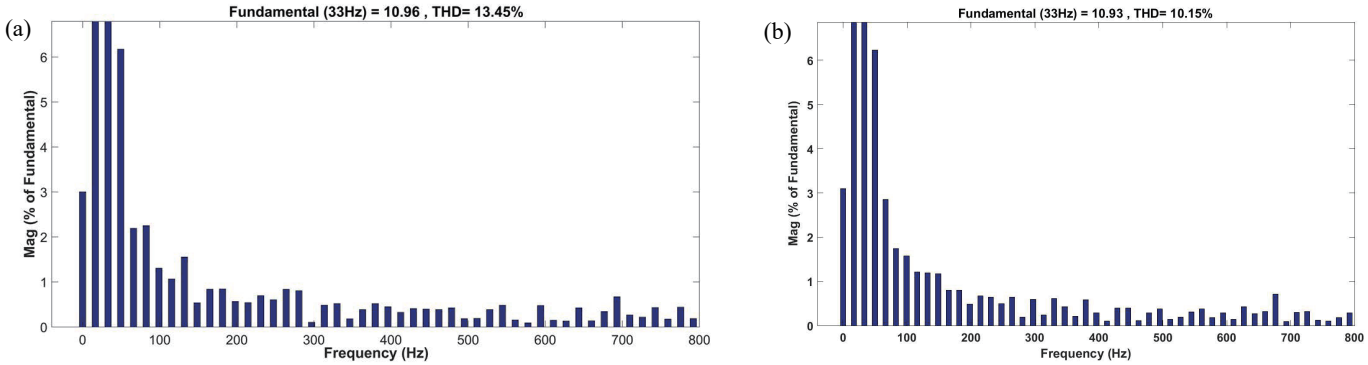

FIGURE 8. THD analysis of A phase stator current. (a) PI. (b) NFTSMC.

cruise of an EV. Fig. 5(a) and Fig. 5(b) show the motor-side and load-side speed response curves, respectively. Fig. 6(a) and Fig. 6(b) show the motor-side and load-side angular position response curves, respectively. Fig. 7(a) and Fig. 7(b) show the motor-side and load-side angular acceleration response curves, respectively. Fig. 8(a) and Fig. 8(b) show the current total harmonic distortion (THD).

Figure 5(a) shows that there is significant torsional vibration on the motor side of the two-inertia system, and the three methods have a certain degree of acceleration delay during the start-up condition. Due to the large torsional stiffness and torsional damping of the system, the torsional vibration of NFTSMC is also relatively obvious compared to conventional SMC with PI control. It can be seen from Fig. 5(b) that the NFTSMC and conventional SMC with load speed feedback can effectively suppress the torsional vibration of EV and the problem of acceleration delay it solved. However, when PI control is used, the torsional vibration on the load side is still obvious, which seriously affects the ride comfort of EV.

Figures 6(a) and 6(b) show that the NFTSMC method has minimal effect on the position angle between the motor and load sides of the two-inertia system compared with conventional SMC and PI control. The method has strong position tracking and minimal effect on the stability of EV at starting and cruising states.

Figures 7(a) and 7(b) show the unstable fluctuation of angular acceleration on the motor side and smoother angular acceleration on the load side. The angular acceleration controlled

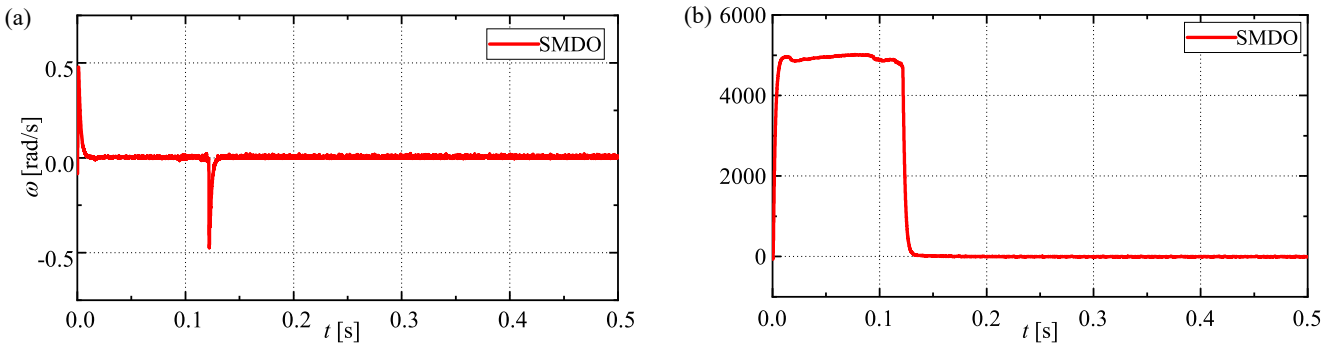

FIGURE 9. Speed tracking error and observed load disturbance. (a) e_ω. (b) $\hat{T}_L$.

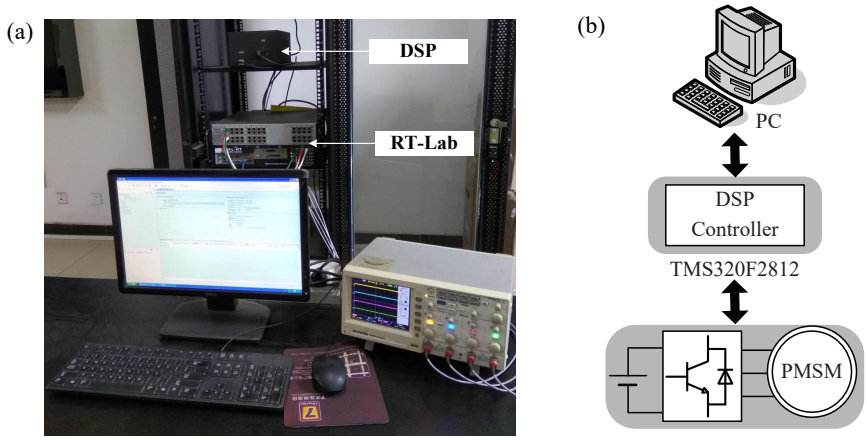

FIGURE 10. RT-LAB HILS experiment platform. (a) RT-LAB platform. (b) Configuration.

by the NFTSMC on the motor side and load side is smaller than that controlled by the PI control and conventional SMC. It maintains high stability at the starting and cruising state.

Figure 8 shows the total harmonic distortion (THD) of the A phase current by PI and NFTSMC control at uniform acceleration conditions. From the THD analysis of phase A in Fig. 8, it can be seen that the phase current THD by PI control is 13.45%, while the proposed NFTSMC algorithm is only 10.15%.

4.3. Simulation Results of SMDO

Figure 9 shows the results of the speed tracking error and the observed load disturbance by using the SMDO.

Figure 9(a) shows that the SMDO has a good tracking performance, and there is no significant observation error in the SMDO during the steady state. As can be seen in Fig. 9(b), the load disturbance portion of the waveform observed by the SMDO is relatively smooth.

4.4. Results of Experiments

To further demonstrate the effectiveness of the presented SMDO-based NFTSMC method, the HILS of the PMSM drive system is carried out on the RT-LAB hardware platform [24, 25]. The HILS platform and configuration are shown in Fig. 10(a) and Fig. 10(b). The experimental parameters are the same as the simulation ones.

Figure 11 shows the d-axis and q-axis current, speed, and torque waveforms by PI control, conventional SMC and NFTSMC algorithm. It is clear from Fig. 11 that compared with PI control and conventional SMC methods, the proposed NFTSMC method can achieve lower torque pulsation and thus reduce the torsional vibration on the load side of the system.

Figure 12 shows the speed and angular position waveforms of the motor and load side for the chattering suppression comparison of the three methods. It is clear from Fig. 12 that the NFTSMC method has a suppressive effect on the load-side torsional vibration and can accurately maintain a stable speed tracking while reducing the motor output torque.

In summary, in comparison with PI control, the conventional SMC and proposed NFTSMC vibration suppression methods can not only accurately track the rotational speed, but also accurately track the rotational speed. The load side has a significant torsional vibration suppression effect in contrast to the severe torsional vibration on the motor side.

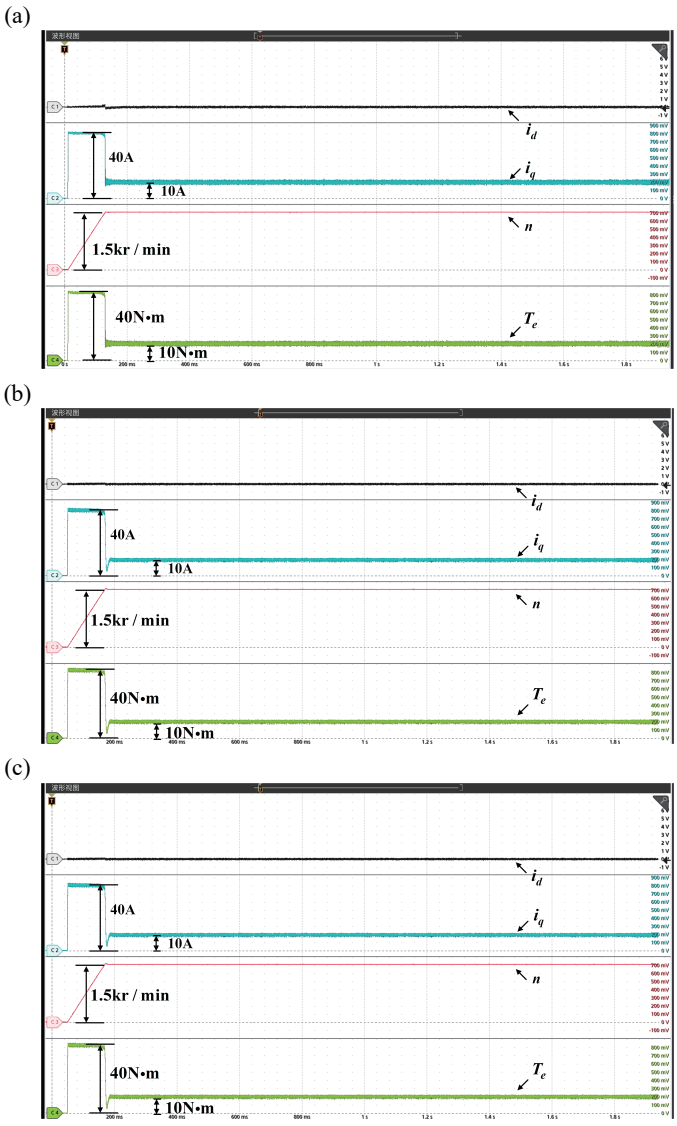

FIGURE 11. Experimental waveforms of the current, speed and torque. (a) PI. (b) SMC. (c) NFTSMC.

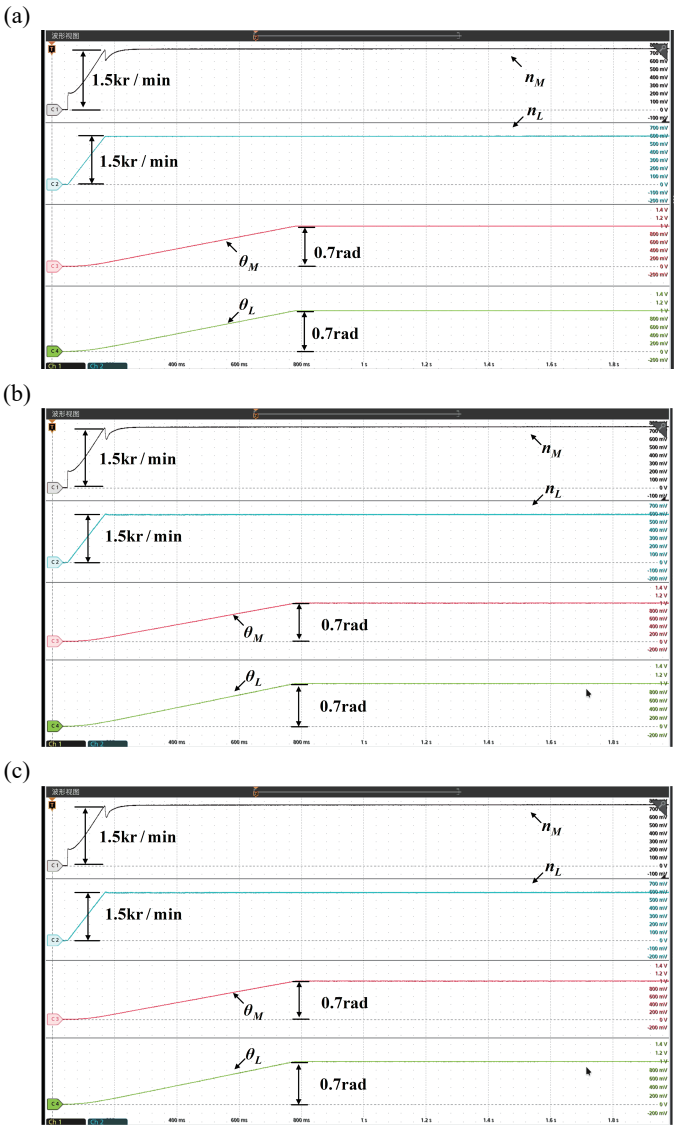

FIGURE 12. Experimental waveforms of the speed and angular position of the motor side and load side. (a) PI. (b) SMC. (c) NFTSMC.

5. CONCLUSION

For the torsional vibration of a PM synchronous drive system under load disturbance, this paper proposes a non-singular fast terminal sliding mode control (NFTSMC) algorithm based on a sliding mode disturbance observer (SMDO). Through simulation and experimental comparison with PI and conventional SMC control methods, the following conclusions are drawn:

(i) The PM synchronous drive system is simplified as two-inertia model. The NFTSMC is designed to suppress the torsional vibration for the PM synchronous drive system. The speed, current, and torque of the motor are quickly converged to the specified values under load disturbance. It ensures the stability of the entire system.

(ii) The SMDO is designed to accurately observe the load disturbance of the permanent magnet drive system. The estimated disturbance is fed forward to compensate the NFTSMC. It effectively suppresses the current and torque pulsation and ensures the high control performance of the permanent magnet drive train.

(ii) The suppression effect on the load-side torsional vibration is achieved by comparing the motor-side and load-side speed, angular acceleration, and angular displacement of the two-inertia system. It verified the correctness and effectiveness of the presented control algorithm.

ACKNOWLEDGEMENT

This work was supported by the National Natural Science Foundation of China under Grant Number (52172403, 62173137), Natural Science Foundation of Hunan Province Number (2023JJ50193, 2023JJ30214, 2023JJ50196), and the Teaching Reform Research Project of Hunan Provincial Education Department of China under Grant HNJG-2022-0847.

REFERENCES

[1] Ahn, K., E. Bayrak, and P. Papalambros, "Electric vehicle design optimization: Integration of a high-fidelity interior-permanent-magnet motor model," *IEEE Transactions on Vehicular Technology*, Vol. 64, No. 9, 3870–3877, 2015.

[2] Zhang, Y., T. Ma, and X. Lu, "Mode optimization of the motor controller cover in a new energy vehicle and its vibration noise analysis," *Journal of Vibration and Shock*, Vol. 41, No. 14, 271–279, 2022.

[3] Zhuang, Y., Y. Wu, B. Zhang, and W. Hu, "Torque coordinated control of distributed drive electric vehicle based on nonlinear MPC," *Journal of Vibration and Shock*, Vol. 40, No. 13, 239–246, 2021.

[4] Tang, X., X. Hu, W. Yang, and H. Yu, "Novel torsional vibration modeling and assessment of a power-split hybrid electric vehicle equipped with a dual-mass flywheel," *IEEE Transactions on Vehicular Technology*, Vol. 67, No. 3, 1990–2000, 2018.

[5] Tang, X., W. Yang, X. Hu, and D. Zhang, "A novel simplified model for torsional vibration analysis of a series-parallel hybrid electric vehicle," *Mechanical Systems and Signal Processing*, Vol. 85, 329–338, 2016.

[6] Li, W., Y. Lu, D. Guo, Y. Liu, X. Shi, and H. Yan, "Mechanical resonance analysis and suppression method of multi-inertia servo system considering time-varying meshing stiffness," *Journal of Vibration and Shock*, Vol. 40, No. 19, 164–171, 2021.

[7] Liu, H., Y. Zhang, X. Li, and S. Liu, "Investigation and restraining of impact torsional vibration of rolling mill's nonlinear drive system," *Journal of Vibration and Shock*, Vol. 29, No. 7, 179–183, 2010.

[8] Yang, Y., J. Zhang, G. Xu, S. Wang, and F. Wang, "Application research onspeed negative feedback in mechanical resonance suppression in servo system," *Transactions of China Electrotechnical Society*, Vol. 33, No. 12, 5459–5469, 2018.

[9] Yu, J., Y. Feng, and J. Zheng, "Suppression of mechanical resonance based on higher-order sliding mode and acceleration feedback," *Control Theory and Applications*, Vol. 26, No. 10, 1133–1136, 2009.

[10] Girsang, I., J. Dhupia, E. Muljadi, M. Singh, and J. Jonkman, "Modeling and control to mitigate resonant load in variable-speed wind turbine drivetrain," *IEEE Journal of Emerging and Selected Topics in Power Electronics*, Vol. 1, No. 4, 277–286, 2013.

[11] Fu, H., G. Tian, H. Chen, and Q. Chen, "A study on the torsional vibration control of motor-transmission integrated drive system," *Automotive Engineering*, Vol. 32, No. 7, 596–600, 2010.

[12] Lv, C., Y. Liu, X. Hu, H. Guo, and D. Cao, "Simultaneous observation of hybrid states for cyber-physical systems: A case study of electric vehicle powertrain," *IEEE Transactions on Cybernetics*, Vol. 48, No. 8, 2357–2367, 2018.

[13] Feng, Y., S. Ren, Q. Chen, and H. Zhao, "Dynamics simulation model of the transmission system for two-speed electric vehicle," *Journal of Mechanical Transmission*, Vol. 37, No. 10, 37–40, 2013.

[14] Vadamalu, R. and C. Beidl, "Mpc for active torsional vibration reduction of hybrid electric powertrains," *IFAC-PapersOnLine*, Vol. 49, 756–761, 2016.

[15] Yu, P., T. Zhang, L. Sun, and R. Guo, "Powertrain torsional vibration study of central-driven pure EV," *Journal of Vibration and Shock*, Vol. 34, No. 10, 121–127, 2015.

[16] Ge, S., Y. Yang, D. Guo, Z. Zhang, and Y. Yi, "Research on dynamic characteristics of electromechanical coupling of electric drive system of electric vehicle," *Journal of Chongqing University of Technology (Natural Science)*, Vol. 35, No. 5, 121–127, 2021.

[17] Zhao, K., W. Dai, R. Zhou, A. Leng, W. Liu, P. Qiu, G. Huang, and G. Wu, "Novel model-free sliding mode control of permanent magnet synchronous motor based on extended sliding mode disturbance observer," *Proceedings of the CSEE*, Vol. 42, No. 6, 2375–2386, 2022.

[18] Zhao, K., W. Liu, Z. Liu, L. Jia, and G. Huang, "Model-free high sliding mode control for permanent magnet synchronous motor," *Transactions of China Electrotechnical Society*, Vol. 38, No. 6, 1472–1485, 2023.

[19] Yang, K., Y. Hu, H. Wu, J. Zhou, W. Xiao, and N. Wang, "Harmonic vibration suppression of maglev rotor system under variable rotational speed without speed measurement," *Mechatronics*, Vol. 91, 11, May 2023.

[20] Zhu, Q., J. Wang, H. Liu, Y. Zhu, and F. Zhang, "Double vibration suppression of PMSM servo system based on strong tracking of reference trajectory," *Journal of Vibration Engineering & Technologies*, 11, 2023.

[21] Wang, X. and H. Zhu, "Vibration compensation control of bpmsm with dead-time effect based on adaptive neural network band-pass filter," *IEEE Transactions on Power Electronics*, Vol. 37, No. 6, 7145–7155, Jun 2022.

[22] Liu, W., H. He, F. Sun, and H. Wang, "Optimal design of adaptive shaking vibration control for electric vehicles," *Vehicle System Dynamics*, Vol. 57, No. 1, 134–159, 2019.

[23] Xu, B., L. Zhang, and W. Ji, "Improved non-singular fast terminal sliding mode control with disturbance observer for PMSM drives," *IEEE Transactions on Transportation Electrification*, Vol. PP, No. 4, 2753–2762, 2021.

[24] Zhao, K., R. Zhou, J. She, C. Zhang, J. He, G. Huang, and X. Li, "Demagnetization-fault reconstruction and tolerant-control for PMSM using improved SMO-based equivalent-input-disturbance approach," *IEEE/ASME Transactions on Mechatronics*, Vol. 27, No. 2, 701 – 712, 2022.

[25] Zhao, K., N. Jia, J. She, W. Dai, R. Zhou, W. Liu, and X. Li, "Robust model-free super-twisting sliding-mode control method based on extended sliding-mode disturbance observer for PMSM drive system," *Control Engineering Practice*, Vol. 139, 105657, 2023.